Observation and Alteration of Surface States of Hematite Photoelectrodes

ARTICLE *in* THE JOURNAL OF PHYSICAL CHEMISTRY C · MARCH 2014

Impact Factor: 4.77 · DOI: 10.1021/jp5006346

6 AUTHORS, INCLUDING:

Chun Du
Boston College, USA
10 PUBLICATIONS **235** CITATIONS
SEE PROFILE

Ji-Wook Jang
Helmholtz-Zentrum Berlin
52 PUBLICATIONS **1,132** CITATIONS
SEE PROFILE

THE JOURNAL OF PHYSICAL CHEMISTRY C

Article

pubs.acs.org/JPCC

Observation and Alteration of Surface States of Hematite Photoelectrodes

Chun Du,[†] Ming Zhang,[‡] Ji-Wook Jang,[†] Yang Liu,[‡] Gang-Yu Liu,*[,‡] and Dunwei Wang*[,†]

[†]Department of Chemistry, Merkert Chemistry Center, Boston College, Chestnut Hill, Massachusetts 02467, United States

[‡]Department of Chemistry, University of California, Davis, California 95616, United States

Supporting Information

ABSTRACT: Hematite prepared by atomic layer deposition (ALD) was found to exhibit photocurrents when illuminated by near-infrared light (λ = 830 nm), whose energy is smaller than the band gap of hematite. The phenomenon was inferred to be a result of valence band to surface state transition. The influence of surface states on the thermodynamics of the hematite/water interface was studied under open-circuit conditions. It was discovered that the equilibrium potential of the hematite surface was more negative than water oxidation potential by at least 0.4 V. With a $NiFeO_x$ coating by photochemical decomposition of organometallic precursors, the equilibrium potential of hematite was restored to water oxidation potential, and the photoresponse under 830 nm illumination was annihilated. Therefore, the states were rationalized by the chemical status at the electrode surfaces, and this hypothesis was supported by similar observations on other metal oxide electrodes such as TiO_2.

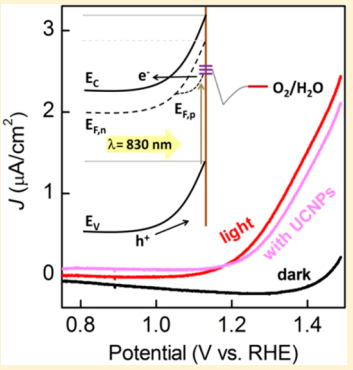

1. INTRODUCTION

Semiconductor-based photocatalytic and photoelectrochemical reactions promise a solar energy storage solution by storing the harvested energy in energetic chemicals such as hydrogen or hydrocarbons.[1−5] The light-to-charge conversion of these reactions is enabled by the development of a built-in field within the semiconductor. Surface states of energies within the band gap often act to reduce the built-in field and, hence, the overall energy conversion efficiency.[6,7] Detailed knowledge and measurements of these surface states would facilitate the effort to construct the electrodes to minimize their negative influence. Although several optical and electrochemical spectroscopic studies on the kinetics and dynamics of surface states on metal oxides in water have been recently reported, the focus has largely been on charge transfer characteristics.[8−10] Little is studied or known regarding the states' impact on thermodynamics, especially at the semiconductor/solution interface. Furthermore, variations in photoelectrode materials, electrolytes, and the time scale during which states were examined make it difficult to attain the structural and chemical origins of these states, which is essential to developing effective mitigations.[11]

To date, an understanding about the nature of surface states on metal oxide photoelectrodes that can be generally applied to a range of materials is unavailable. Treatments remain empirical. Here, we report a progress toward filling the voids. In the context of water oxidation by hematite (α-Fe_2O_3), we confirmed the existence of surface states and their negative impacts on the measurable photovoltage (V_{ph}). The states are consistent with a chemical origin at surfaces, which can be readily oppressed by facile $NiFeO_x$ surface treatments. This understanding permitted us to predict and alter the surface states of a similar nature on TiO_2 photoelectrodes, which was not reported previously.

The prototypical material of hematite represents an earth-abundant compound whose band gap promises a potentially high solar-to-hydrogen conversion efficiency (up to 16%).[12−15] Hematite materials also present many challenges, e.g., poor light absorption near the band edge, short hole diffusion distance, and slow charge transfer kinetics. These properties found in various other metal oxides are all present in hematite, making it a good research tool to test material design and treatment strategies that are of generic importance. One particular challenge of hematite pertaining to surface states is the low V_{ph} generation, typically <0.4 V.[16,17] The consequence is manifested by the late turn-on characteristics in the current-density−voltage (J−V) plots. Recent studies by us confirmed that low V_{ph}, not high overpotential requirement, is the reason for the late turn-on.[18] Here we focus our study on the origin of the low V_{ph}.

Using hematite in water as an example, Figure 1 depicts how surface states contribute to reduce V_{ph} and provides a good starting point to address the thermodynamic aspects of the system. We note that the influence of the surface states in other aspects such as possible increase of charge transfer kinetics across the hematite/water interface is not considered, to enable the focus on thermodynamics. The distance between the Fermi level (electronegativity of the material, χ) and conduction band

Special Issue: Michael Grätzel Festschrift

Received: January 19, 2014
Revised: March 23, 2014

   dx.doi.org/10.1021/jp5006346 | J. Phys. Chem. C XXXX, XXX, XXX−XXX

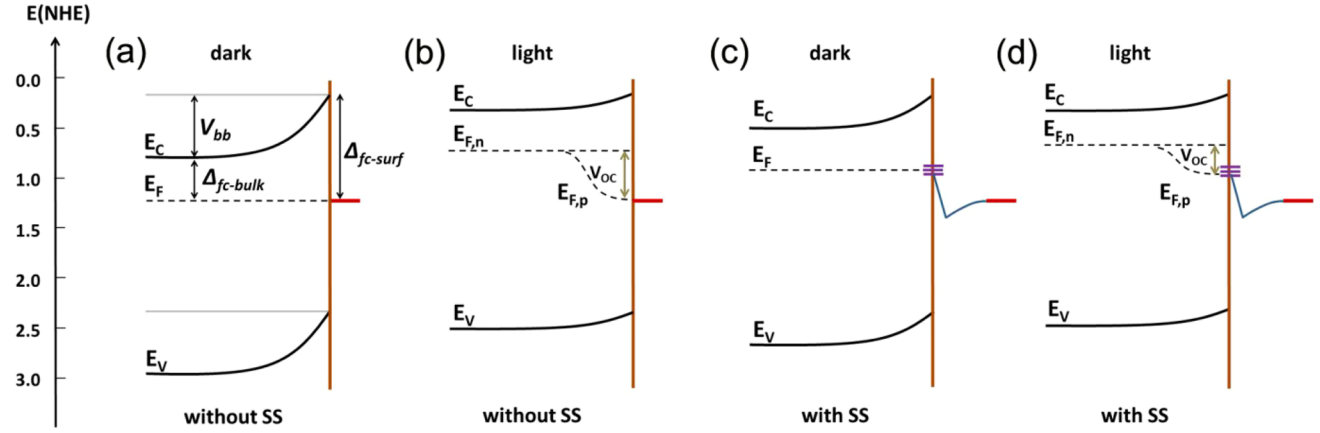

Figure 1. Band diagrams of hematite in water under open-circuit conditions with and without surface states (SS). (a) In the absence of light and SS, the degree of band bending (V_{bb}) is determined by the difference of Fermi level and conduction band edge in the body and that on the surface (see eq 1 in the main text). (b) Under illumination, photogenerated charges split the Fermi levels of electrons ($E_{F,n}$) and holes ($E_{F,p}$) and produce a photovoltage on the surface, which is equal to or smaller than V_{bb}. (c) Surface states contribute to pinning the Fermi level relative to the band edge positions, reducing the degree of band bending. (d) Illuminated hematite with surface states produces a smaller V_{ph}. See main text for more discussions.

minimum (electron affinity of the material, EA) is defined as Δ_{fc} ($\Delta_{fc} = \chi - EA$). The degree of band bending (V_{bb}) is then defined by $\Delta_{fc\text{-}surf}$ and $\Delta_{fc\text{-}bulk}$ following eq 1.[19]

$$V_{bb} = \Delta_{fc\text{-}surf} - \Delta_{fc\text{-}bulk} \quad (1)$$

V_{bb} sets the thermodynamic limit of the achievable V_{ph}. If the doping level of a semiconductor is given, $\Delta_{fc\text{-}bulk}$ would be fixed. To maximize V_{ph}, one would have to increase $\Delta_{fc\text{-}surf}$. The existence of surface states is detrimental to V_{ph} because it reduces $\Delta_{fc\text{-}surf}$ by pinning χ relative to EA (Figure 1d). Alternatively, under the condition of complete band edge pinning, the difference between χ in vacuum and the electrochemical potential of the solution (E_{sol}) defines $\Delta_{fc\text{-}surf}$, which in turn determines V_{bb}. The surface states unpin band edges relative to E_{sol}, reducing $\Delta_{fc\text{-}surf}$ and, ultimately, V_{ph} (Figures 1c and 1d).

The influence of surface states on hematite performance has been reported previously. For instance, Sivula and Grätzel et al. have shown that an ultrathin coating of Al_2O_3 by atomic layer deposition (ALD) onto hematite improves its photoelectrochemical performance.[20] The effect was attributed to surface state passivation. Bisquert and Hamman et al. examined the energetics and density of surface states on hematite by electrochemical impedance spectroscopy under illumination.[9] These observations, however, were made under conditions far away from the thermodynamic equilibrium, with surface O_2 evolution chemistry already established. It is unclear how the chemical reactions may alter the nature of the surface. Our goal for this work is to provide new insights about the surface states under conditions at or close to thermodynamic equilibrium. First, direct observations are made to demonstrate the existence of the surface states. Next, the surface states are examined under conditions close to thermodynamic equilibrium. Finally, a hypothesis was made regarding the nature of the states, which is proven effective in predicting surface states of other metal oxide systems that have not been reported previously.

2. EXPERIMENTAL SECTION

2.1. FTO Substrate Preparation. FTO substrates were purchased from Sigma-Aldrich (~8 Ω/sq). Prior to the ALD growth of hematite, the FTO substrate was diced into 1 × 1 cm^2 pieces and cleaned with acetone, methanol, isopropanol, and deionized (DI) water, sequentially. The cleaning process was concluded by a 10 min sonication in DI water (Branson 1510).

2.2. ALD Growth of Hematite and TiO_2 Thin Films. Both hematite (25 nm) and TiO_2 (20 nm) thin films were grown by ALD on conductive FTO substrates. The details of ALD hematite growth were reported by us previously.[16,17,21] Briefly, iron *tert*-butoxide ($Fe_2(^tBuO)_6$, heated at 120 °C) and H_2O (room temperature) were used as an Fe and O precursor, respectively. The substrate temperature was maintained in an ALD chamber (Savannah Cambridge Nanotech) at 180 °C with 20 sccm (standard cubic centimeters per minute) N_2 flow as the carrier gas. Each ALD growth cycle consisted of an Fe precursor pulse (5 s) and exposure (15 s), a 10 s purge of N_2, a water pulse (0.05 s), exposure (15 s), and another 10 s purge of N_2. The condition was found to yield a growth rate of ca. 0.5 Å/cycle. The synthesis was concluded by a calcination treatment in air at 500 °C for 20 min. TiO_2 growth was carried out following a protocol reported by us.[22] Briefly, Ti ($^iPrO)_4$ (heated at 75 °C) was used as the precursor for Ti, and H_2O (room temperature) was used as the precursor for O. The substrate was heated to 275 °C during the growth. A growth rate of 0.3 Å was maintained. Both hematite and TiO_2 produced by this method are inherently n-type.

2.3. Surface Structure Characterizations. The morphologies of the as-grown hematite film and FTO substrates were observed by a Hitachi S-4100T field emission scanning electron microscope (FESEM) and an Asylum Research Corp. MFP-3D atomic force microscope (AFM). All AFM images were acquired via contact mode with imaging force of 15−20 nN. Silicon probes MSNL-10 with a force constant of 0.1 N/m were purchased from Bruker (Camarillo, CA). The AFM images were acquired and analyzed using Asylum MFP3D software developed on the Igor Pro 6.12 platform.

2.4. $NiFeO_x$ Preparation. $NiFeO_x$ was deposited by a photochemical decomposition technique reported by Smith et al.[23] Briefly, iron(III) 2-ethylhexanoate ($C_{16}H_{30}FeO_4$, 50% Fe in mineral spirits, Strem Chemicals) and nickel(II) 2-ethylhexanoate ($Ni[OOCCH(C_2H_5)C_4H_9]_2$, 78% Ni in 2-ethylhexanoic acid, Strem Chemicals) were mixed in an appropriate

dx.doi.org/10.1021/jp5006346 | J. Phys. Chem. C XXXX, XXX, XXX−XXX

amount of hexane with a 1:1 ratio to produce a solution with 15% (wt %) metal complex. For each deposition, 10 μL of mixing precursor solution was drop-casted on the photoelectrode surface using a liquid transfer gun. Afterward, the electrode with $NiFeO_x$ was irradiated with UV light (UVO cleaner 42) for 3 h. The process was completed by an annealing in ambient atmosphere at 100 °C for 1 h.[18]

2.5. Photoelectrochemical Measurements. After ALD growth, hematite or TiO_2-covered substrates were connected to copper wires with conductive silver epoxy (Allied Electronics). The entire substrates, other than the photoactive front sides, were then covered by nonconductive hysol epoxy (Loctite). All photoelectrochemical (PEC) measurements were performed on a CHI 604C Potentiostat/Galvanostat in a three-electrode configuration, with a Pt wire as the counter electrode and Hg/HgO in 1 M NaOH as the reference electrode (for solutions whose pH was lower than 12, Ag/AgCl in 1 M KCl was used as a reference electrode). Solutions with different pH values were prepared as follows. A solution of 1 M NaOH was used to produce solutions of pH 13.6; 0.2 M phosphate buffer was used to produce solutions of pH 12.3, 10.3, 8.3, and 6.0; 0.2 M acetic acid solution was used to produce solutions of pH 4.9. All pH values were measured by an Orion 4-Star pH meter (Thermo Scientific). Prior to open-circuit potential measurements, O_2 was bubbled into the solution for at least 20 min to ensure the electrolyte was saturated with O_2. The O_2 saturated solution provides a standard/reference to enable accurate determination of open-circuit potential measurements. During the measurements, O_2 flow was maintained. The solution was stirred vigorously during the measurements. Each open-circuit potential reading was obtained after a minimum 30 min stabilization process under open-circuit conditions.

3. RESULTS AND DISCUSSION

3.1. Preparation and Characterization of Hematite Films. Scanning electron micrographs of bare FTO substrates are shown in Figure 2a. Typical FTO domain size ranged from 60 to 80 nm. After ALD growth of hematite, typical domains measured 120 to 150 nm as shown in Figure 2b. AFM images enabled high-resolution visualization of surface features with true topographic height. The height of domains of bare FTO ranged from 6 to 40 nm (Figure 2c,e). The FTO surface was relatively flat with an RMS roughness of 15.4 ± 2.7 nm. Upon ALD growth of hematite, the height was measured from 10 to 70 nm (Figure 2d,f) with RMS roughness of 33.2 ± 1.9 nm. This RMS roughness was obtained from more than ten scans at 2 × 2 μm^2 size. The observed morphology and topography are consistent with known hematite thin films (targeted thickness, 25 nm) prepared under ALD.[16]

3.2. Direct Observation of Surface States on Hematite under IR Light. A direct evidence of the surface states came from the photoresponses of hematite under illumination of infrared (IR) light. When excited at λ = 830 nm, significant photocurrent was detected, as shown in Figure 3a. This response is surprising as the excitation energies (1.5 eV) are far smaller than what is allowed by hematite's band gap (2.1 eV). These responses are reproducible, measured from all eight batches of hematite samples investigated. Spectroscopic analysis of the light source confirmed that no photons with energies greater than E_g of hematite were emitted (Figure S1 in Supporting Information, SI). Therefore, we infer that the absorption is due to transition from the valence band to mid band gap states (inset in Figure 3a), i.e., surface states. These

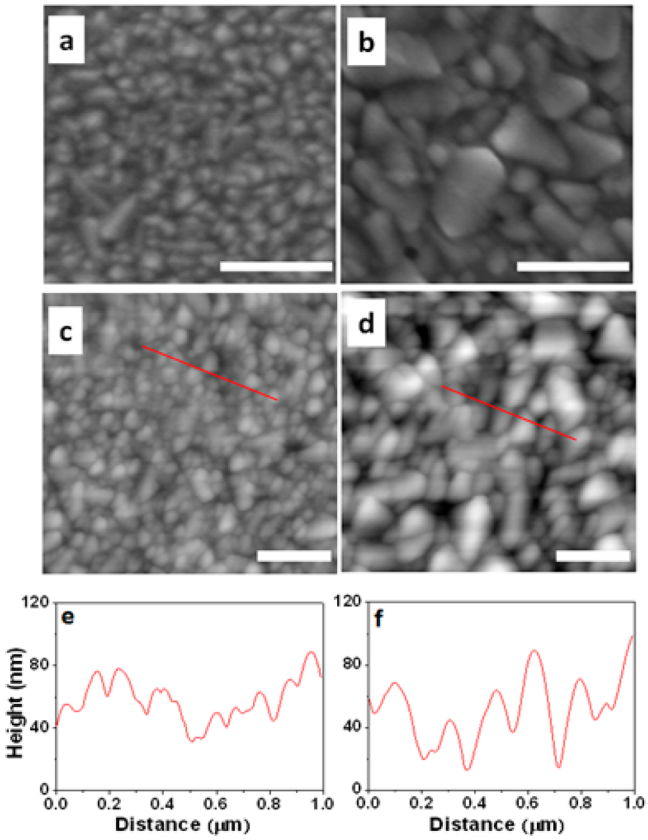

Figure 2. Surface characterization of FTO substrate before (left) and after (right) hematite growth. (a) and (b) are scanning electron micrographs with scale bars of 500 nm. (c) and (d) are 2 × 2 μm^2 AFM topograph images with scale bars at 500 nm. (e) and (f) present the corresponding cursor profiles as indicated in images (c) and (d), respectively.

electrons, however, would not contribute to photocurrents unless they are collected, i.e., reaching conduction band. Two mechanisms may contribute to the collection, two-photon absorption or band-to-band tunneling. Given that the photocurrent at 830 nm illumination was only observed at highly positive potentials and that the hematite film is thin (ca. 20 nm), the band-to-band tunneling mechanism is more likely, as shown in Figure 3a.

The conclusion of surface states is strongly supported by the result shown in Figure 3b, where a known treatment was employed to alter surface states. When the surface of hematite was treated by $NiFeO_x$, which was shown to help alter the influence of surface states,[18] the photoresponse to 830 nm illumination diminished, as shown in Figure 3b. Additional support of surface states came from a comparison to rare earth nanoparticle (REN) covered hematites.[24] Rare-earth-based upconversion nanoparticles (REUCNPs) were known to harvest photons at 980 nm and emit green light (λ = 520 and 550 nm), giving rise to a measurable photocurrent otherwise not observed on bare hematite.[24] The direct excitation at 830 nm yields similar and more prominent responses without REUCNPs (see Figure 3a), which therefore indicates intrinsic properties, e.g., surface states. Final evidence of the surface states came from energetics. Using 6.9 eV as the nominal valence band edge position in vacuum, we obtained the energy levels of the states at ~5.4 eV, which translates to ~0.4 V more negative than water oxidation potential (or ~0.9

dx.doi.org/10.1021/jp5006346 | J. Phys. Chem. C XXXX, XXX, XXX−XXX

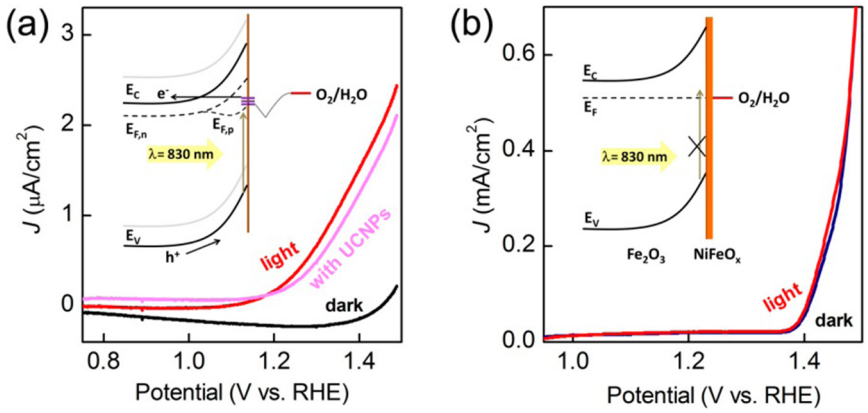

Figure 3. Photoresponse to 830 nm IR light by hematite with and without the influence of surface states. (a) A small but non-negligible photocurrent was consistently measured on bare hematite, with or without REUCNPs. Inset: energy band diagram showing the proposed mechanism for the IR photoresponse. Band edge positions before unpinning (without the applied positive potential) are shown in gray. (b) When the surface of hematite was covered by $NiFeO_x$, the photoresponse was annihilated. Inset: proposed mechanism for the prohibited transition with energy changes smaller than the band gap.

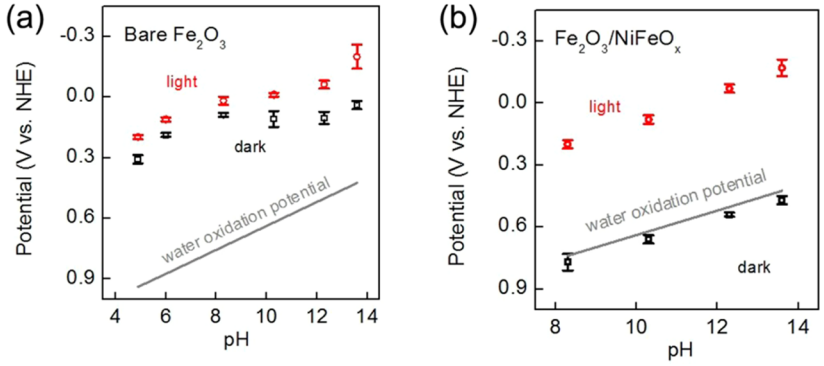

Figure 4. Open-circuit potential measurements of hematite with and without the influence of surface states. (a) The surface states pin the Fermi level and lead to variation of dark OCPs relative to water oxidation potential. The dark OCPs are sensitive to pH and generally are more negative than water oxidation potential by 0.4 V or more. OCPs in light are shown in red. (b) $NiFeO_x$ alters the influence of surface states and restores the dark OCPs to water oxidation potential. The dark OCPs relative to RHE are independent of solution pH.

V vs RHE) after adjusting for the pH and assuming hematite band edge positions are pinned relative to water oxidation potential. We are mindful that accurate quantification of surface states would require a systematic investigation on the photoresponses upon excitations at the full range of radiation. The lack of laser radiations at the full range prevents the required investigations at the scope of this paper. To ascertain the robustness of the observations and surface states, corroborating evidence was collected from thermodynamic measurements discussed in the next section.

3.3. Open-Circuit Potential Measurements on Hematite. In an effort to observe the surface states at or near equilibrium, we probed the electrochemical potential of the hematite photoelectrode under open-circuit conditions in the dark (Figure 4a). When there is no light and no net exchange current between the electrode and the electrolyte, there are no net chemical reactions on the surface. The Fermi level is flat and in equilibrium with the E_{sol}. Measurement of electrode potential (E_{bulk}) reports on the electrochemical potential of the surface (E_{surf}), which in turn is determined by E_{sol}. Although whether E_{surf} is equal to water oxidation potential (1.23 V vs RHE) depends on many factors (e.g., the nature of the surface and O_2 partial pressure in the solution),[25] it is expected to at least track E_{sol}. The change of E_{bulk} should follow the change of E_{sol} (by varying pH, for instance) in a linear fashion. The expectation was met by measurements of $NiFeO_x$-decorated hematite photoelectrodes (Figure 4b). Remarkably, the measured dark OCPs across a wide pH range were at 1.25 ± 0.04 V vs RHE, close to water oxidation potential of 1.23 V vs RHE. The OCPs of bare hematite in the dark, however, were far more negative, by 0.40 V or more, than water oxidation potential. We understand the deviation as a result of surface states, which contribute to pinning the Fermi level. Important to our discussion, the OCP at pH 13.6 (1.0 M NaOH), under which the majority of photoelectrochemical characterizations of hematite was conducted, was +0.85 ± 0.03 V vs RHE. They are approximately 1.6 V above the valence band maximum of hematite, under the likely assumption that the band edge positions of hematite are pinned relative to water redox potentials in highly alkaline solutions. It explains why the bare hematite photoelectrodes produced measurable photocurrents under 830 nm excitation. The energy levels are depicted in Figure 1c,d for easy viewing.

Another feature of the data in Figure 4a is worth emphasizing. The deviation from water oxidation potential varies with pH and reaches the greatest value of 0.65 V at pH = 8.3. The point of zero zeta potential of hematite also occurs at the same pH region (pH = 8.3–8.6).[26] The apparent coincidence points to a likely origin of surface states, i.e., adsorbates on surfaces. With 100 nm of $NiFeO_x$ coating, the

dx.doi.org/10.1021/jp5006346 | J. Phys. Chem. C XXXX, XXX, XXX–XXX

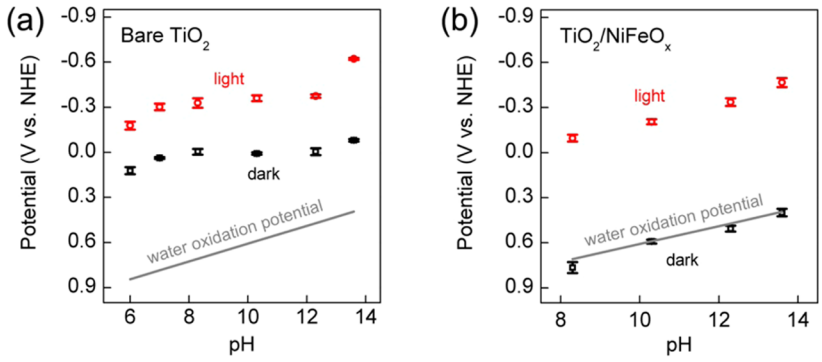

Figure 5. Open-circuit potential measurements of TiO_2 with and without the influence of surface states. (a) The presence of surface states leads to significant deviation of the dark OCPs from water oxidation potential. (b) $NiFeO_x$ coating alters the influence of surface states and restores the dark OCPs to water oxidation potential. OCPs under illumination are shown in red.

influence of surface states is removed, as shown in Figure 4b. The thickness and homogeneity of the coating have been measured using TEM following our prior protocols.[18] This comparison indicates that the surface features at the hematite/water contact are responsible for the surface states. Obvious suspects include adsorbed water (including physisorbed and chemisorbed), other adsorbates, or structural defects of hematite. Our preliminary studies have eliminated some of the factors such as structural defects by using different electrode materials, such as TiO_2 (see next section).

3.4. Open-Circuit Potential Measurements on TiO_2. The data presented in Figure 4 were highly reproducible not only on different samples prepared separately but also in various electrolyte solutions (e.g., with or without buffers of different compositions, see Supporting Information). We hypothesize that the adsorption of an H_2O molecule and its derivatives (OH^- and H^+) is responsible for the surface states studied here. The hypothesis implies that surface states of similar energies may exist on other metal oxide photoelectrodes as well. To test the prediction, TiO_2, an extensively studied photoelectrode material, was utilized. In comparison with hematite, one purported advantage of TiO_2 is its relatively negative Fermi level, which promises high V_{ph} and low V_{on}. Indeed, V_{on} as low as 0.1−0.2 V vs RHE is reported in the literature.[27,28] The low V_{on} makes it seemingly unnecessary to question what is the true V_{ph} by TiO_2. Our prediction based on the afore-described hypothesis is that the dark OCP of TiO_2 would be significantly more negative than water oxidation potential and that the V_{ph} by TiO_2 would be much lower than its band gap of 3.2 eV. We see in Figure 5a that the dark OCPs of TiO_2 are indeed consistently more negative than water oxidation potential by 0.48 V or more. Assuming the dark OCPs report on the surface state energy, we obtained a surface state energy level of +0.78 V vs RHE (pH 13.6), quasi-quantitatively consistent with that obtained on hematite (+0.85 V vs RHE). The result further highlights that the surface states are independent of the substrate composition. They are most likely caused by surface-adsorbed species. When a layer of $NiFeO_x$ was deposited on TiO_2, the dark OCPs were restored to the water oxidation potential. The measured V_{ph} increased from 0.54 V (bare TiO_2) to 0.86 V (with $NiFeO_x$ decoration) at pH 13.6. Also consistent with the result on hematite, the lowest photovoltage by TiO_2 was obtained at pH close to the point of zero zeta potential (see Supporting Information).[29] The apparent coincidence supports that the surface states originate from adsorbates.

4. CONCLUSION

To successfully implement semiconductor-powered photochemisty for applications such as solar fuel production, comprehensive knowledge of the interfaces between the semiconductor and the solution is required. While surface states are generally recognized as a potential source of problems in terms of photovoltage generation, the nature of them remains a topic of debate. Inspired by a surprising observation that hematite produces photocurrent by sub-band gap excitations, we examined the surface state energetics at or near thermodynamic equilibrium. The surface potential of hematite was found to be significantly more negative than water oxidation potential. We concluded that the observation was a direct consequence of surface states at potentials close to +0.85 V vs RHE. These observations in conjunction with the pH dependence of the measured potentials lead to a likely origin of the surface states, i.e., surface adsorbates. The hypothesis was further supported by the observation that surface states of similar energy were present on TiO_2 electrodes. A facile $NiFeO_x$ deposition has proven effective in diminishing the observed changes in photocurrent responses and open-circuit potentials. These results reveal new insights into surface states of hematite and metal oxide electrodes. We hope these initial efforts and findings trigger more experimental investigations into the semiconductor/water interfaces toward a deeper understanding of water splitting processes. Work is in progress toward modification of electrode surfaces via more advanced approaches, such as site-specific modifications and using sub to full monolayers. We also plan to use more localized techniques, such as Kelvin probe microscopy,[30] to study the surface states further.

■ ASSOCIATED CONTENT

Ⓢ Supporting Information

Spectroscopic characterization of the 830 nm light source; photoresponses to 830 nm light at different pH; open-circuit potential measurements of hematite in solutions of different pH, with and without buffer; schematic drawing of open-circuit potential measurement; open-circuit potential measurements of TiO_2 in different pH buffer solutions. This material is available free of charge via the Internet at http://pubs.acs.org.

■ AUTHOR INFORMATION

Corresponding Authors

*E-mail: gyliu@ucdavis.edu. Tel.: (530) 754 9678.
*E-mail: dunwei.wang@bc.edu. Tel.: (617) 552 3121.

dx.doi.org/10.1021/jp5006346 | J. Phys. Chem. C XXXX, XXX, XXX−XXX

Notes

The authors declare no competing financial interest.

■ ACKNOWLEDGMENTS

We thank financial support from the National Science Foundation (DMR 105572, 1317280, to C.D., J.-W.J., and D.W.), American Chemical Society (ACS-PRF-ND, to M.Z. and G.Y.L.), California Energy Commission (EISG 57513A-12-15, to M.Z. and G.Y.L.), and the Alfred P. Sloan Foundation (to D.W.).

■ REFERENCES

(1) Grätzel, M. Photoelectrochemical Cells. *Nature* **2001**, *414*, 338−344.
(2) Turner, J. A. Sustainable Hydrogen Production. *Science* **2004**, *305*, 972−974.
(3) Barton, E. E.; Rampulla, D. M.; Bocarsly, A. B. Selective Solar-Driven Reduction of CO_2 to Methanol Using a Catalyzed p-GaP Based Photoelectrochemical Cell. *J. Am. Chem. Soc.* **2008**, *130*, 6342−6344.
(4) Walter, M. G.; Warren, E. L.; McKone, J. R.; Boettcher, S. W.; Mi, Q.; Santori, E. A.; Lewis, N. S. Solar Water Splitting Cells. *Chem. Rev.* **2010**, *110*, 6446−6473.
(5) Lin, Y.; Yuan, G.; Liu, R.; Zhou, S.; Sheehan, S. W.; Wang, D. Semiconductor Nanostructure-Based Photoelectrochemical Water Splitting: A Brief Review. *Chem. Phys. Lett.* **2011**, *507*, 209.
(6) Bard, A. J.; Faulkner, L. R. *Electrochemical Methods: Fundamental and Applications*; John Wiley & Sons: New York, 1980.
(7) Yang, X.; Du, C.; Liu, R.; Xie, J.; Wang, D. Balancing Photovoltage Generation and Charge-Transfer Enhancement for Catalyst-Decorated Photoelectrochemical Water Splitting: A Case Study of the Hematite/MnO_x Combination. *J. Catal.* **2013**, *304*, 86−91.
(8) Barroso, M.; Mesa, C. A.; Pendlebury, S. R.; Cowan, A. J.; Hisatomi, T.; Sivula, K.; Grätzel, M.; Klug, D. R.; Durrant, J. R. Dynamics of Photogenerated Holes in Surface Modified α-Fe_2O_3 Photoanodes for Solar Water Splitting. *Proc. Natl. Acad. Sci. U.S.A.* **2012**, *109*, 15640−15645.
(9) Klahr, B.; Gimenez, S.; Fabregat-Santiago, F.; Hamann, T.; Bisquert, J. Water Oxidation at Hematite Photoelectrodes: The Role of Surface States. *J. Am. Chem. Soc.* **2012**, *134*, 4294−4302.
(10) Huang, Z.; Lin, Y.; Xiang, X.; Rodríguez-Córdoba, W.; McDonald, K. J.; Hagen, K. S.; Choi, K.-S.; Brunschwig, B. S.; Musaev, D. G.; Hill, C. L. In Situ Probe of Photocarrier Dynamics in Water-Splitting Hematite (α-Fe_2O_3) Electrodes. *Energy Environ. Sci.* **2012**, *5*, 8923−8926.
(11) Gamelin, D. R. Water Splitting: Catalyst or Spectator? *Nat. Chem.* **2012**, *4*, 965−7.
(12) Sivula, K.; Le Formal, F.; Grätzel, M. Solar Water Splitting: Progress Using Hematite (α-Fe_2O_3) Photoelectrodes. *ChemSusChem* **2011**, *4*, 432−449.
(13) Lin, Y.; Yuan, G.; Sheehan, S.; Zhou, S.; Wang, D. Hematite-Based Solar Water Splitting: Challenges and Opportunities. *Energy Environ. Sci.* **2011**, *4*, 4862−4869.
(14) Katz, M. J.; Riha, S. C.; Jeong, N. C.; Martinson, A. B.; Farha, O. K.; Hupp, J. T. Toward Solar Fuels: Water Splitting with Sunlight and "Rust"? *Coord. Chem. Rev.* **2012**, *256*, 2521−2529.
(15) Mayer, M. T.; Lin, Y.; Yuan, G.; Wang, D. Forming Heterojunctions at the Nanoscale for Improved Photoelectrochemical Water Splitting by Semiconductor Materials: Case Studies on Hematite. *Acc. Chem. Res.* **2013**, *46*, 1558−1566.
(16) Lin, Y.; Xu, Y.; Mayer, M. T.; Simpson, Z.; MacMahon, G.; Zhou, S.; Wang, D. Growth of p-type Hematite by Atomic Layer Deposition and Its Utilization for Improved Solar Water Splitting. *J. Am. Chem. Soc.* **2012**, *134*, 5508.
(17) Mayer, M. T.; Du, C.; Wang, D. Hematite/Si Nanowire Dual-Absorber System for Photoelectrochemical Water Splitting at Low Applied Potentials. *J. Am. Chem. Soc.* **2012**, *134*, 12406−12409.
(18) Du, C.; Yang, X.; Mayer, M. T.; Hoyt, H.; Xie, J.; McMahon, G.; Bischoping, G.; Wang, D. Hematite-Based Water Splitting with Low Turn-On Voltages. *Angew. Chem., Int. Ed.* **2013**, *52*, 12692−12695.
(19) Bisquert, J.; Cendula, P.; Bertoluzzi, L.; Gimenez, S. Energy Diagram of Semiconductor/Electrolyte Junctions. *J. Phys. Chem. Lett.* **2014**, *5*, 205−207.
(20) Le Formal, F.; Tétreault, N.; Cornuz, M.; Moehl, T.; Grätzel, M.; Sivula, K. Passivating Surface States on Water Splitting Hematite Photoanodes with Alumina Overlayers. *Chem. Sci.* **2011**, *2*, 737−743.
(21) Lin, Y.; Zhou, S.; Sheehan, S. W.; Wang, D. Nanonet-Based Hematite Heteronanostructures for Efficient Solar Water Splitting. *J. Am. Chem. Soc.* **2011**, *133*, 2398−2401.
(22) Lin, Y.; Zhou, S.; Liu, X.; Sheehan, S.; Wang, D. TiO_2/$TiSi_2$ Heterostructures for High-Efficiency Photoelectrochemical H_2O Splitting. *J. Am. Chem. Soc.* **2009**, *131*, 2772−2773.
(23) Smith, R. D.; Prévot, M. S.; Fagan, R. D.; Zhang, Z.; Sedach, P. A.; Siu, M. K. J.; Trudel, S.; Berlinguette, C. P. Photochemical Route for Accessing Amorphous Metal Oxide Materials for Water Oxidation Catalysis. *Science* **2013**, *340*, 60−63.
(24) Zhang, M.; Lin, Y.; Mullen, T. J.; Lin, W. F.; Sun, L. D.; Yan, C. H.; Patten, T. E.; Wang, D.; Liu, G. Y. Improving Hematite's Solar Water Splitting Efficiency by Incorporating Rare-Earth Upconversion Nanomaterials. *J. Phys. Chem. Lett.* **2012**, *3*, 3188−3192.
(25) Pleskov, Y. V. *Solar Energy Conversion: A Photoelectrochemical Approach*; Springer-Verlag: New York, 1990.
(26) Butler, M.; Ginley, D. Prediction of Flatband Potentials at Semiconductor - Electrolyte Interfaces from Atomic Electronegativities. *J. Electrochem. Soc.* **1978**, *125*, 228−232.
(27) Hwang, Y. J.; Hahn, C.; Liu, B.; Yang, P. Photoelectrochemical Properties of TiO_2 Nanowire Arrays: A Study of the Dependence on Length and Atomic Layer Deposition Coating. *ACS Nano* **2012**, *6*, 5060−5069.
(28) Wang, G.; Wang, H.; Ling, Y.; Tang, Y.; Yang, X.; Fitzmorris, R. C.; Wang, C.; Zhang, J. Z.; Li, Y. Hydrogen-Treated TiO_2 Nanowire Arrays for Photoelectrochemical Water Splitting. *Nano Lett.* **2011**, *11*, 3026−3033.
(29) Preocanin, T.; Kallay, N. Point of Zero Charge and Surface Charge Density of TiO2 in Aqueous Electrolyte Solution as Obtained by Potentiometric Mass Titration. *Croat. Chem. Acta* **2006**, *79*, 95−106.
(30) Halpern, E.; Elias, G.; Kretinin, A. V.; Shtrikman, H.; Rosenwaks, Y. Direct Measurement of Surface States Density and Energy Distribution in Individual In As Nanowires. *Appl. Phys. Lett.* **2012**, *100*, 262105.